

# Interpretation of (Pu,U) matrix effect on atomization of analytes during GF-AAS analysis

Neelam Goyal<sup>a</sup>, Renu Agarwal<sup>b</sup>, Paru J. Purohit<sup>a</sup>, S.V. Godbole<sup>a,\*</sup>

<sup>a</sup> Radiochemistry Division, Radiochemistry and Isotope Group, Bhabha Atomic Research Centre, Mumbai 400 085, India

<sup>b</sup> Product Development Section, Radiochemistry and Isotope Group, Bhabha Atomic Research Centre, Mumbai 400 085, India

Received 3 December 2007; accepted 20 February 2008

## Abstract

Atomization of Al, Cr, Cu, Cs, Mn, Ni and Sr in (Pu,U) matrix was studied and the effect of Pu/(Pu + U) composition of the matrix on analyte absorbance was investigated. The changes observed in the absorbance signals for the analytes with change in composition of (Pu,U) matrix were correlated with relative oxygen partial pressures of the analyte oxides, UO<sub>2</sub>, PuO<sub>2</sub> and the purge gas. The studies were utilised for the direct determination of trace levels of these analytes in (Pu,U) matrix containing 25 at.% Pu by graphite furnace atomic absorption spectrometry (GF-AAS) with a relative precision of approximately ±10%.

© 2008 Elsevier B.V. All rights reserved.

## 1. Introduction

An atomic absorption spectrometric with graphite atomizer (GF-AAS) is one of the sensitive and specific methods for trace metal determination. Atomic emission spectrometry (AES) [1] methods using inductively coupled plasma (ICP) and d.c. arc are capable of providing multi element analysis after chemical separation and carrier distillation respectively, of the analytes from the (Pu,U) matrix, and unlike GF-AAS technique they need gram quantities of samples. GF-AAS being a sensitive and precise technique, offers an alternative analytical method for nuclear materials requiring only µg amounts of samples. Studies reported [2,3] previously for the determination of impurities in radioactive samples by GF-AAS involved their chemical separation from the matrix. GF-AAS methods have been reported from our laboratory for the determination of trace elements in the nuclear fuels viz. uranium [4], thorium [5], (Pu,U) mixed oxide [6–8] and in other materials, e.g., graphite [9] and Al–U [10]. It was observed

that absorbance of the trace amounts of analytes was dependent upon matrix composition. Reports are also available for the elemental determination of analytes in a radiological environment using Flame AAS [11–14].

The mechanism of release of gaseous atom from the solid lattice in GF-AAS has been investigated by thermodynamics – kinetics approaches [15]. The aim of this study is to understand the change in the analyte absorbance signals with the change in composition of (Pu,U) matrix in GF-AAS. It is to be noted that though nitrate solution of analyte with uranyl and plutonium nitrate is loaded, nitrates get converted to oxides of analyte, U and Pu. These analytes have to be released from U and Pu oxides. Hence, thermodynamic calculations were carried out to determine equilibrium partial pressure of oxygen at various temperatures for analyte oxide, uranium oxide and plutonium oxide. A comparison of partial oxygen pressures of the purge gas with oxides of the matrix elements (Pu/U) and analytes was used to understand the matrix composition effect on absorbance signals. These studies were utilized for direct determination of wppm amounts of Al, Cr, Cu, Cs, Mn, Ni and Sr in (Pu,U) matrix containing 25 at.% Pu by GF-AAS, for fast breeder reactor fuels.

\* Corresponding author. Tel.: +91 22 25594578; fax: +91 22 25505151.  
E-mail address: [svgod@barc.gov.in](mailto:svgod@barc.gov.in) (S.V. Godbole).

## 2. Experimental

A modular type Varian Techtron AA-6 Atomic Absorption Spectrometer with pyrolytically coated mini Massman carbon rod atomizer (CRA-63) was used in these investigations. Glove box adapted Varian Techtron AA-6 atomic absorption spectrometer provides absorption measurements in peak height mode and all the measurements were carried out in peak height mode. The details of modifications of the instrument and the operating current of hollow cathode lamps (HCL), the spectral bandwidth, the spectral line used for each element, the preparation of plutonium (40 mg/ml) and uranium (200 mg/ml) solution along with detailed procedure followed have been described elsewhere [6,7]. Argon gas of purity 99.995 vol.% was used as a purge gas.

To study the matrix effect, the (Pu,U) composition was varied in the range 0–100 at.% Pu, viz. 10, 37.5, 50, 75 and 100 at.% while keeping the total (Pu,U) concentration in the solution fixed at 20 mg/ml. For direct determination of the above mentioned analytes in (Pu,U) matrix with Pu/(Pu + U) = 0.25, a series of standard solutions were prepared. The analytes' concentrations were varied from 0 to 500 ng/ml, except for caesium and aluminium, for which the range was 0–1 µg/ml and 0–10 µg/ml, respectively. Initially the absorbance for a fixed concentration of the analyte was measured as a function of Pu/(Pu + U) composition for a total concentration of 20 mg/ml on a uranium conditioned atomizer. Absorbances were then measured by successively increasing Pu content.

Due to the non-availability of well-established standards with Pu matrix, three synthetic samples in (Pu,U) matrix were prepared, by spiking ICP multi element standard IV, MERCK containing 23 elements for evaluation of the precision and accuracy of the method developed here. The analytical response was determined for each of the analytes and the analysis of the synthetic samples was carried out using the standard procedure.

## 3. Results and discussion

In GF-AAS, atomization of an analyte in the presence of matrix is the result of an interaction of analyte–matrix,

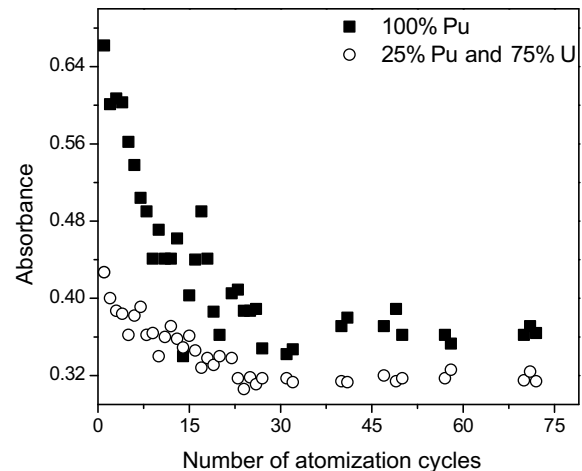


Fig. 1. Influence of matrix build-up in atomizer on absorbance of 5 wppm of Mn (a). 100 at.% Pu (b). 25 at.% Pu + 75 at.% U.

analyte–carbon or carbon–matrix. The atomization of these analytes was studied in presence of Pu/U by measuring the atomic absorption signal for each of the element in the absence as well as presence of the matrix. Successive loadings of the (Pu,U) samples and standards leads to matrix build up inside the graphite tube. Typical results obtained for one of the analyte, Mn, in matrices containing 25 at.% Pu and 100 at.% Pu with number of atomization cycles are shown in Fig. 1. A reduction of absorbance was observed, with accumulation of 3 mg matrix in 30 atomization cycles, which was followed by a stable signal up to 70 atomization cycles and beyond. Similar reduction in analyte signals was noted for Al, Cr, Cs, Cu, Ni and Sr for initial 30 atomization cycles. These investigations stress the importance of conditioning the atomizer by loading 3 mg of matrix. Subsequent investigations are, therefore, carried out on conditioned atomizer. Pre-atomization temperature and time duration were 900 °C and 40 s, respectively, for all these analytes. Optimized experimental parameters used for determination of these analytes are given in Table 1.

The variation in GF-AAS absorbance signal of different analytes as a function of increase in Pu percentage in

Table 1

Optimized experimental parameters, analytical results and Characteristic concentration for the determination of Al, Cr, Cu, Cs, Mn, Ni and Sr in (Pu,U) matrix

Element	Atomization temperature (°C)	Duration (s)	Linear analytical range in (Pu,U) matrix wppm <sup>a</sup>	Determination limit (g)	Characteristic concentration <sup>**</sup> (ng/ml)		
					Aqueous [6]	U [6]	25 at.%Pu
Al	2700	4	10–500	$1.0 \times 10^{-9}$	9.0	–	71
Cr	2400	3	0.5–10	$5.0 \times 10^{-11}$	1.8	4.2	2.0
Cu	2400	3	0.5–10	$5.0 \times 10^{-11}$	1.7	4.9	2.3
Cs	2550	3	2.5–50	$2.5 \times 10^{-10}$	0.87	–	8.7
Mn	2550	3	0.5–20	$5.0 \times 10^{-11}$	2.1	5.0	3.0
Ni	2550	4	1.0–20	$1.0 \times 10^{-10}$	2.0	13.9	7.0
Sr	2700	4	0.5–25	$5.0 \times 10^{-11}$	0.27	–	1.8

<sup>a</sup> Based on 100 µg of plutonium–uranium in 5 µl of solution.

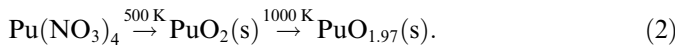
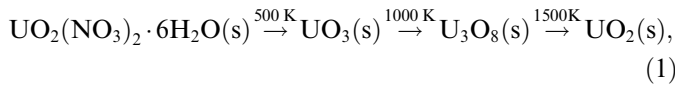
<sup>\*\*</sup> Characteristic concentration is defined as the concentration corresponding to an absorbance of 0.0044.

Table 2  
Data on the effect of plutonium on absorbance values for Al, Cr, Cu, Cs, Mn, Ni and Sr in (Pu,U) matrix

Element	Conc. (wppm)	(Pu,U) matrix composition					
		Pure U	(Pu <sub>0.1</sub> U <sub>0.9</sub> )	(Pu <sub>0.37</sub> U <sub>0.63</sub> )	(Pu <sub>0.5</sub> U <sub>0.5</sub> )	(Pu <sub>0.75</sub> U <sub>0.25</sub> )	Pure Pu
Al	5	0.667	0.574	0.444	0.348	0.358	0.340
Cr	0.1	0.174	0.221	0.335	0.439	0.454	0.475
Cu	0.1	0.334	0.436	0.491	0.652	0.718	0.715
Cs	0.5	0.902	0.999	1.151	1.351	1.434	1.415
Mn	0.04	0.076	0.095	0.110	0.131	0.165	0.167
Ni	0.2	0.434	0.455	0.576	0.610	0.675	0.693
Sr	0.2	0.828	0.556	0.513	0.384	0.368	0.324

(Pu,U) matrix is given in Table 2. A continuous increase in absorbance was observed for Cr, Cu, Cs, Mn and Ni with progressive increase in Pu percentage whereas, Al and Sr showed reverse trend. Since GF-AAS provides only indirect information of the processes occurring in a graphite atomizer; we tried to explain the change in analyte atomization with change in matrix compositions with relative oxygen partial pressures of the analyte oxides, uranium oxide and plutonium oxide.

Thermogravimetric analysis [16,17] shows decomposition of uranyl and plutonium nitrates to respective dioxides in the temperature range 500–1500 K as follows:



Therefore, by the time the system reaches a temperature of 1500 K, both uranium and plutonium nitrates get converted into their respective dioxides. Both UO<sub>2</sub> and PuO<sub>2</sub> thus formed are very stable lattices. Similarly, the analytes also get converted into their oxides, mostly dissolved in the main lattice of (Pu,U)O<sub>2</sub>. The diffusion rates of cationic elements in these lattices are very low [18–20]. Moreover, very small amounts of the analytes dissolved in (Pu,U)O<sub>2</sub> lattice considerably reduce their chemical activities, hence their detectability. Therefore, these cationic analytes are trapped in the lattice of (Pu,U)O<sub>2</sub>. To understand the trend observed in the present atomic absorption studies while changing the Pu/(Pu + U) fraction of the matrix, it is important to understand the process by which these analytes get released from the matrix. The oxides of the analytes in (Pu,U)O<sub>2</sub> matrix were formed by decomposition of the nitrate solutions loaded on a graphite atomizer in the presence of flowing argon as a purge gas. In the presence of argon atmosphere, the graphite generated a reducing atmosphere for all the analytes as well as for (Pu,U)O<sub>2</sub>. The order of reduction of the analyte as well as matrix oxides depends on their partial oxygen pressure. An argon gas of purity 99.995 vol.%, with the assumption of oxygen as the only impurity, has a p<sub>O<sub>2</sub></sub> ≈ 5.0 Pa at low temperatures, when there is no reaction between graphite and oxygen. However, at atomization temperatures, oxygen will react with graphite to give a dynamic equilibrium between C–

O<sub>2</sub>–CO–CO<sub>2</sub>–O [15]. The partial oxygen pressure of this system was calculated using Gibbs energies of formation of CO, CO<sub>2</sub> and O given in Table 3. The equilibrium equations used for the calculations were as follows:

$$p_{CO_2} = p_{O_2} \exp\left(\frac{-\Delta_f G_{CO_2}^0}{RT}\right), \quad (3)$$

$$p_{CO} = p_{O_2}^{1/2} \exp\left(\frac{-\Delta_f G_{CO}^0}{RT}\right), \quad (4)$$

$$p_O = p_{O_2}^{1/2} \exp\left(\frac{-\Delta_f G_O^0}{RT}\right). \quad (5)$$

where p<sub>CO</sub>, p<sub>CO<sub>2</sub></sub>, p<sub>O<sub>2</sub></sub> and p<sub>O</sub> are the partial pressures of CO, CO<sub>2</sub>, O<sub>2</sub> and O, respectively and Δ<sub>f</sub>G<sub>CO</sub><sup>0</sup>, Δ<sub>f</sub>G<sub>CO<sub>2</sub></sub><sup>0</sup>, Δ<sub>f</sub>G<sub>O</sub><sup>0</sup> are the Gibbs energies of formation of CO, CO<sub>2</sub> and O, respectively. The total amount of oxygen in these chemical species was fixed by the amount of oxygen impurity in argon atmosphere; therefore, the following constraint was imposed:

$$0.5x_{CO} + x_{CO_2} + x_{O_2} + 0.5x_O = \text{oxygen in argon}. \quad (6)$$

The mole fraction of the various gaseous components (x<sub>i</sub>) is related to their partial pressures (p<sub>i</sub>) and the total pressure (P<sub>tot</sub>) by the following relation:

$$p_{CO} = x_{CO}P_{tot}; \quad p_{CO_2} = x_{CO_2}P_{tot}; \quad p_{O_2} = x_{O_2}P_{tot}; \quad p_O = x_OP_{tot}. \quad (7)$$

Table 3  
Gibbs energies of formation of relevant oxides (Δ<sub>f</sub>G<sup>0</sup> = A + BT log(T) + CT)

Formation reaction	Δ <sub>f</sub> G <sup>0</sup> (J/mol)			Reference
	A	B	C	
½ O <sub>2</sub> (g) = O (g)	252950	0	-65.8	[22]
C (s) + O <sub>2</sub> (g) = CO <sub>2</sub> (g)	-392521	4.97	-18.3	[22]
C (s) + ½ O <sub>2</sub> (g) = CO (g)	-113998	0	-85.4	[22]
2Al(l) + 3/2 O <sub>2</sub> (g) = Al <sub>2</sub> O <sub>3</sub> (s)	-1698836	-15.70	386.1	[21]
2Cr(s) + 3/2 O <sub>2</sub> (g) = Cr <sub>2</sub> O <sub>3</sub> (s)	-1121016	0	260.0	[21]
2Cs(l) + ½ O <sub>2</sub> (g) = Cs <sub>2</sub> O (s)	-321580	0	101.5	[22]
2Cu(s) + ½ O <sub>2</sub> (g) = Cu <sub>2</sub> O (s)	-169565	-16.41	123.5	[21]
Mn(s) + ½ O <sub>2</sub> (g) = MnO (s)	-399421	0	82.5	[21]
Ni (s) + ½ O <sub>2</sub> (g) = NiO (s)	-244718	0	98.6	[21]
Sr (l) + ½ O <sub>2</sub> (g) = SrO (s)	-592570	0	102.8	[22]
U (l) + O <sub>2</sub> (g) = UO <sub>2</sub> (s)	-1129180	-64.48	406.1	[21]
Pu (l) + O <sub>2</sub> (g) = PuO <sub>2</sub> (s)	-1039959	0	180.7	[22]

As the total pressure of the purge gas was approximately 0.1 MPa the mole fractions of the gaseous species were equal to their partial pressures. By substituting Eqs. (3)–(5) and the above equalities in the Eq. (6), the following expression for partial pressure of oxygen was obtained:

$$p_{O_2} + p_{O_2} \exp\left(\frac{-\Delta_f G_{CO_2}^0}{RT}\right) + 0.5p_{O_2}^{1/2} \exp\left(\frac{-\Delta_f G_{CO}^0}{RT}\right) + 0.5p_{O_2}^{1/2} \exp\left(\frac{-\Delta_f G_{O}^0}{RT}\right) = \text{oxygen in Ar.} \quad (8)$$

The partial pressure of oxygen over the atomizer was calculated from Eq. (8) and its substitution in Eqs. (3)–(5) gave the partial pressures of CO<sub>2</sub>, CO, O and O<sub>2</sub>, as given in Table 4. The partial pressure of oxygen in the purge gas was also calculated by assuming air to be impurity in argon, therefore, the oxygen content of the argon was  $1 \times 10^{-3}$  vol.% and these recalculated  $p_{O_2}$  values are also given in Table 4. The small difference in oxygen partial pressures calculated for the two impurity contents did not affect the interpretation of our results. The partial oxygen pressures of all the relevant metal oxides were calculated from their respective Gibbs energies of formation, listed in Table 3. The variation of oxygen pressures of these oxides along with oxygen pressure of the purge gas as a function of temperature are plotted in Fig. 2. Graphite furnace is highly dynamic and open system and one can argue that estimation of partial pressure of oxygen based on equilibrium thermodynamic calculations is inappropriate. However, these calculations represent micro-equilibrium in the system in dynamic conditions and are indicative of the observed trends of the reactions at different temperatures. If at any selected temperature, the partial oxygen pressure of the purge gas is lower than that of a metal oxide then that oxide will get reduced to metal. Whereas, metal oxides

with partial oxygen pressures lower than that of the purge gas will remain as oxides. As can be seen from Fig. 2, most of the analytes, Cu, Ni, Cs, Cr and Mn get reduced at temperatures much lower than that of PuO<sub>2</sub> or UO<sub>2</sub>. The temperature of reduction of (Pu,U)O<sub>2</sub> solution matrix will be between the reduction temperatures of UO<sub>2</sub> and PuO<sub>2</sub>, depending on the composition of (Pu,U)O<sub>2</sub>. The higher the plutonium content of the matrix, lower will be the reduction temperature of that matrix. The highly reduced activity of the analyte oxides by dissolution in (Pu,U)O<sub>2</sub> matrix will result in trapping the analytes till the (Pu,U)O<sub>2</sub> lattice breaks down by reduction to (Pu,U) metal phase. As PuO<sub>2</sub> reduces at lower temperature than UO<sub>2</sub>, the increase in PuO<sub>2</sub> content of (Pu,U)O<sub>2</sub> matrix will reduce the temperature of breaking down of the oxide lattice and hence increase the detectability of the analytes. This explains the increase in absorbance values of Cu, Ni, Cs, Cr and Mn with increase in Pu/(Pu + U) content of the solution. However, aluminium and strontium showed reverse trend. As can be seen from the Fig. 2, partial pressures of oxygen of Al<sub>2</sub>O<sub>3</sub> and SrO are lower than that of PuO<sub>2</sub>. Whereas,  $p_{O_2}$  of UO<sub>2</sub> is higher than that of Al<sub>2</sub>O<sub>3</sub> but lower than that of SrO. Therefore, PuO<sub>2</sub> and Pu-rich (Pu,U)O<sub>2</sub> will be reduced to metal before reduction of Al<sub>2</sub>O<sub>3</sub>. Whereas, (Pu,U)O<sub>2</sub> of any composition will be reduced to metal phase before the reduction of SrO. Hence, the main lattice will be a liquid metal phase while analytes will be present as Al<sub>2</sub>O<sub>3</sub> and SrO. When these analytes get reduced to metals, their activity will be greatly reduced by dissolution in the liquid metal phase (Pu,U). An increase in plutonium content of the matrix, decreases the temperature of appearance of (Pu,U) liquid phase, resulting in decreased activity of Al and Sr due to their dissolution in the metal phase.

The analytical results namely linear analytical range and limit of determination for these analytes in presence of (Pu,U) matrix are given in Table 1. The atomization tem-

Table 4  
Partial pressures of various oxygen carrying species in the purge gas

T (K)	$5.0 \times 10^{-3}$ vol.% O <sub>2</sub> in Ar				$10^{-3}$ vol.% O <sub>2</sub> in Ar
	$p_{O_2}$ (Pa)	$p_{CO}$ (Pa)	$p_{CO_2}$ (Pa)	$p_O$ (Pa)	$p_{O_2}$ (Pa)
1000	$1.5 \times 10^{-24}$	10.1	$7.2 \times 10^{-4}$	$2.5 \times 10^{-34}$	$6.0 \times 10^{-26}$
1100	$1.8 \times 10^{-23}$	10.1	$1.2 \times 10^{-4}$	$4.8 \times 10^{-32}$	$7.2 \times 10^{-25}$
1200	$1.4 \times 10^{-22}$	10.1	$2.5 \times 10^{-5}$	$3.9 \times 10^{-30}$	$5.8 \times 10^{-24}$
1300	$8.4 \times 10^{-22}$	10.1	$7.0 \times 10^{-6}$	$1.6 \times 10^{-28}$	$3.3 \times 10^{-23}$
1400	$3.8 \times 10^{-21}$	10.1	$2.3 \times 10^{-6}$	$3.8 \times 10^{-27}$	$1.5 \times 10^{-22}$
1500	$1.4 \times 10^{-20}$	10.1	$8.8 \times 10^{-7}$	$5.9 \times 10^{-26}$	$5.6 \times 10^{-22}$
1600	$4.4 \times 10^{-20}$	10.1	$3.8 \times 10^{-7}$	$6.6 \times 10^{-25}$	$1.7 \times 10^{-21}$
1700	$1.2 \times 10^{-19}$	10.1	$1.8 \times 10^{-7}$	$5.5 \times 10^{-24}$	$4.8 \times 10^{-21}$
1800	$2.9 \times 10^{-19}$	10.1	$9.3 \times 10^{-8}$	$3.7 \times 10^{-23}$	$1.2 \times 10^{-20}$
1900	$6.5 \times 10^{-19}$	10.1	$5.1 \times 10^{-8}$	$2.0 \times 10^{-22}$	$2.6 \times 10^{-20}$
2000	$1.3 \times 10^{-18}$	10.1	$3.0 \times 10^{-8}$	$9.1 \times 10^{-22}$	$5.4 \times 10^{-20}$
2100	$2.6 \times 10^{-18}$	10.1	$1.9 \times 10^{-8}$	$3.6 \times 10^{-21}$	$1.0 \times 10^{-19}$
2200	$4.7 \times 10^{-18}$	10.1	$1.2 \times 10^{-8}$	$1.3 \times 10^{-20}$	$1.9 \times 10^{-19}$
2300	$8.1 \times 10^{-18}$	10.1	$8.0 \times 10^{-9}$	$4.0 \times 10^{-20}$	$3.2 \times 10^{-19}$
2400	$1.3 \times 10^{-17}$	10.1	$5.5 \times 10^{-9}$	$1.1 \times 10^{-19}$	$5.3 \times 10^{-19}$
2500	$2.1 \times 10^{-17}$	10.1	$3.9 \times 10^{-9}$	$3.0 \times 10^{-19}$	$8.4 \times 10^{-19}$
2600	$3.2 \times 10^{-17}$	10.1	$2.9 \times 10^{-9}$	$7.2 \times 10^{-19}$	$1.3 \times 10^{-18}$

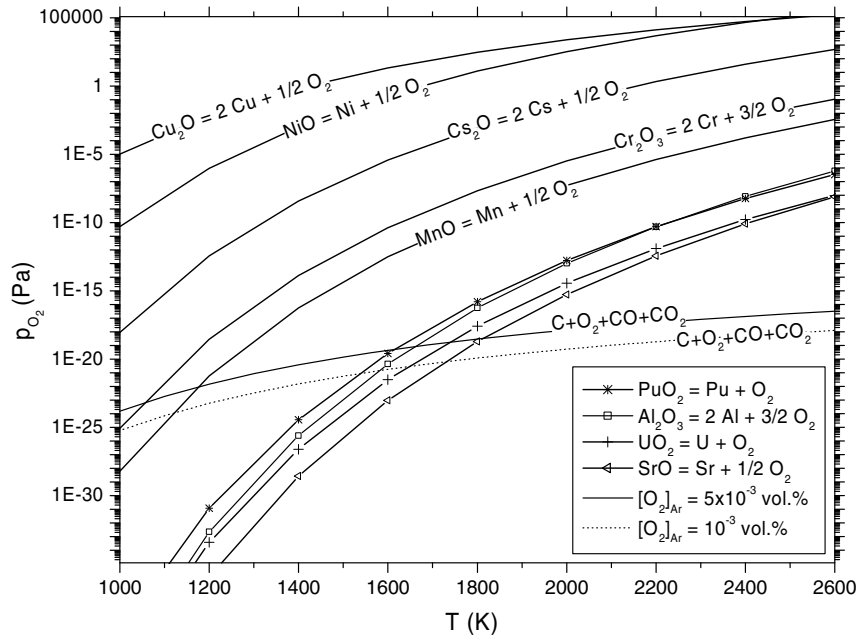


Fig. 2. A comparison of oxygen partial pressures of different oxides with that of the purge gas as a function of temperature.

peratures given in Table 1 are more representative than being the absolute values but they indicate the trend in which these analytes were detected. The above explanation of breaking down of the oxide lattice structure also explains the appearance of Sr and Al at higher temperature than other analytes as their oxides get reduced at much higher temperatures. The characteristic concentrations obtained for all analytes in (Pu,U) matrix at 25 at.% Pu solution, as evaluated from calibration plots, are shown in Table 1 along with those reported for aqueous and ura-

nium matrices. The reproducibility of analyte determination was estimated by repetitive analyses of the synthetic samples (Table 5) and is in good agreement with the spiked amounts with a precision of  $\pm 10\%$  RSD. This indicates that the presence of 16 other common metallics at trace levels does not show any measurable effect on the determination of these analytes.

#### 4. Conclusion

The increase in absorbance observed for Cr, Cu, Cs, Mn and Ni with increase in Pu content in (Pu,U) matrix was attributed to lower partial oxygen pressure of  $\text{UO}_2$  than that of  $\text{PuO}_2$ . The lower oxygen partial pressure of (Pu,U) $\text{O}_2$  results in higher temperature of conversion of oxide matrix into metal phase. The suppressive effect observed in Al and Sr in plutonium rich matrices is correlated with reduction in their activities by dissolution in liquid metal phase. From these results it can be concluded that the elements forming oxides with partial oxygen pressures higher than either  $\text{UO}_2$  or  $\text{PuO}_2$  are expected to show increase in absorbance with increase in plutonium content of the matrix. Whereas, elements that make oxides with partial oxygen pressures lower than  $\text{PuO}_2$  are expected to show decrease in absorbance with increase in plutonium content. In the same analogy it can be concluded that the presence of a very stable intermetallic compound between analyte and the lattice element will also reduce the appearance of that analyte in vapor phase. The graphite furnace atomic absorption spectrometric method described here can be applied for direct determination of wppm level impurities of Al, Cr, Cu, Cs, Mn, Ni and Sr in (Pu,U) matrix containing 25 at.% Pu with a relative precision of about  $\pm 10\%$ .

Table 5  
Results of analyses of three synthetic samples for the determination of Al, Cr, Cu, Cs, Mn, Ni and Sr in (Pu,U) matrix with 25 at.% Pu

Element	Amount added wppm	Amount determined wppm	% RSD
Al	15	14	8.4
	75	77	7.6
	200	185	4.5
Cr	2.5	2.4	6.2
	4.0	4.2	4.9
	7.5	8.1	5.2
Cu	2.5	2.6	9.0
	4.0	4.3	3.5
	7.5	8.1	2.9
Cs	4.0	4.1	4.3
	7.5	6.9	3.8
	20.0	20.0	3.1
Mn	2.5	2.6	8.0
	4.0	3.8	5.0
	7.5	7.2	3.0
Ni	2.5	2.4	7.1
	7.5	7.5	6.1
	15.0	15.3	3.8
Sr	1.5	1.6	5.3
	7.5	7.5	4.1
	20.0	19.0	2.9

## Acknowledgements

Authors are grateful to Dr. V.K. Manchanda, Head, Radiochemistry Division and Mr. B.K. Sen, Head, Product Development Section, for their encouragement and support during the course of this work.

## References

- [1] A.A. Argekar, M.J. Kulkarni, J.N. Mathur, A.G. Page, *Talanta* 56 (2002) 591.
- [2] G. Baudin, *Prog. Analyt. Atom. Spectrosc.* 3 (1980) 3.
- [3] L.E. Cox, USAEC Report LA-5791, 1974.
- [4] N. Goyal, P.J. Purohit, A.R. Dhobale, B.M. Patel, A.G. Page, M.D. Sastry, *J. Anal. Atom. Spectrom.* 2 (1987) 459.
- [5] N. Goyal, M.J. Kulkarni, S.K. Thulasidas, P.J. Purohit, A.G. Page, *Anal. Lett.* 32 (1999) 3059.
- [6] N. Goyal, P.J. Purohit, A.R. Dhobale, A.G. Page, M.D. Sastry, *Fresenius J. Anal. Chem.* 330 (1988) 114.
- [7] N. Goyal, P.J. Purohit, A.G. Page, M.D. Sastry, *Fresenius J. Anal. Chem.* 354 (1996) 311.
- [8] N. Goyal, P.J. Purohit, A.G. Page, *Fresenius J. Anal. Chem.* 361 (1998) 429.
- [9] N.K. Porwal, S.K. Thulasidas, S.V. Godbole, P.J. Purohit, N. Goyal, A.G. Page, *Anal. Lett.* 29 (1996) 821.
- [10] N. Goyal, P.J. Purohit, A.G. Page, M.D. Sastry, *Talanta* 39 (1992) 775.
- [11] S.A. Barker, S.G. Johnson, G.C. Knighton, M.T. Sayer, B.M. Candee, V.D. Dimick, *Appl. Spectrosc.* 50 (1996) 816.
- [12] N. Goyal, P.J. Purohit, B.A. Dhawale, A.G. Page, *Chem. Environ. Res.* 13 (2004) 233.
- [13] M. Ganivet, A. Benhmou, *Anal. Chim. Acta* 47 (1969) 81.
- [14] J. Vienney, *Anal. Chim. Acta* 55 (1971) 37.
- [15] S.B. Chang, C.L. Chakrabarti, *Prog. Analyt. Atom. Spectrosc.* 8 (1985) 102, and reference therein.
- [16] C. Duval, *Inorganic Thermogravimetric Analysis*, Elsevier, New York, 1963, pp. 666, 659.
- [17] J.M. Cleaveland, *Chemistry of Plutonium*, Gordon & Breach, New York, 1970.
- [18] T.A. Lauritzen, P.E. Novak, J.H. Davies, USAEC Report GEAP-4466, General Electric Company, March 1966.
- [19] Hj. Matzke, *J. Nucl. Mater.* 114 (1983) 121.
- [20] D. Glasser-Leme, Hj. Matzke, *J. Nucl. Mater.* 106 (1982) 211.
- [21] O. Kubaschewski, C.B. Alcock, *Metallurgical Thermochemistry*, 5th Ed., Pergamon, New York, 1979.
- [22] G.V. Belov, B.G. Trusov, ASTD, *Computer-aided Reference-book in Thermodynamical, Thermochemical and Thermophysical Properties of Species*, Version 2.0, © 1983–1995, Moscow.